

RESEARCH

Open Access

# Cytosolic $\text{Ca}^{2+}$ shifts as early markers of cytotoxicity

Philippe Wyrsch<sup>†</sup>, Christian Blenn<sup>†</sup>, Theresa Pesch, Sascha Beneke and Felix R Althaus<sup>\*</sup>

## Abstract

The determination of the cytotoxic potential of new and so far unknown compounds as well as their metabolites is fundamental in risk assessment. A variety of strategic endpoints have been defined to describe toxin-cell interactions, leading to prediction of cell fate. They involve measurement of metabolic endpoints, bio-energetic parameters or morphological cell modifications. Here, we evaluated alterations of the free cytosolic  $\text{Ca}^{2+}$  homeostasis using the Fluo-4 dye and compared results with the metabolic cell viability assay Alamar Blue. We investigated a panel of toxins ( $\text{As}_2\text{O}_3$ , gossypol,  $\text{H}_2\text{O}_2$ , staurosporine, and titanium(IV)-salane complexes) in four different mammalian cell lines covering three different species (human, mouse, and African green monkey). All tested compounds induced an increase in free cytosolic  $\text{Ca}^{2+}$  within the first 5 s after toxin application. Cytosolic  $\text{Ca}^{2+}$  shifts occurred independently of the chemical structure in all tested cell systems and were persistent up to 3 h. The linear increase of free cytosolic  $\text{Ca}^{2+}$  within the first 5 s of drug treatment correlates with the  $\text{EC}_{25}$  and  $\text{EC}_{75}$  values obtained in Alamar Blue assays one day after toxin exposure. Moreover, a rise of cytosolic  $\text{Ca}^{2+}$  was detectable independent of induced cell death mode as assessed by caspase and poly(ADP-ribose) polymerase (PARP) activity in HeLa versus MCF-7 cells at very low concentrations. In conclusion, a cytotoxicity assay based on  $\text{Ca}^{2+}$  shifts has a low limit of detection (LOD), is less time consuming (at least 24 times faster) compared to the cell viability assay Alamar Blue and is suitable for high-throughput-screening (HTS).

**Keywords:** Alamar blue, Arsenic trioxide, Fluo-4, Gossypol,  $\text{H}_2\text{O}_2$ , Staurosporine

## Background

The development of assays estimating the cytotoxic potential of drugs and chemicals is of fundamental interest in early risk assessment to prioritize them for further testing. Moreover, a few years ago, the European Union (EU) initiated a regulation for the Registration, Evaluation and Authorisation of Chemicals (REACH). Around 30 000 chemical substances, which are manufactured, imported or, used in the EU require validation [1,2]. The implementation of REACH will increase the demand of cytotoxicity testing and risk assessment.

In the past, a variety of different biological endpoints have been defined for cytotoxicity testing. These include the assessment of energy status (ATP depletion, ATP/ADP ratio), cell membrane integrity (Neutral red, Trypan blue, lactate dehydrogenase (LDH) leakage), DNA-strand

breaks (COMET) as well as metabolic parameters (3-(4,5-Dimethylthiazol-2-yl)-2,5-diphenyltetrazolium bromide (MTT), Alamar Blue) [3-5]. The evaluation of these parameters is often time and cost intensive and several different endpoints must be considered for a final decision.

The determination of metabolic activity using the Alamar Blue viability assay is based on mitochondrial hydrolase activity that is generally affected by many different drugs as well as radiation [6-8]. Blue resazurin is metabolized into pink resorufin by viable cells and this color change quantifies the amount of intact cells (Figure 1A). Here, we evaluated the toxicity of four model compounds in adherent cell cultures from three different species: human cervical (HeLa) and breast cancer cells (MCF-7), murine fibroblasts and kidney epithelial cells from African green monkey (Vero 76) (Figure 2A, B). We compared the cytotoxicity of arsenic trioxide ( $\text{As}_2\text{O}_3$ ), gossypol, hydrogen peroxide ( $\text{H}_2\text{O}_2$ ) and staurosporine in Alamar Blue assays with toxin-induced elevations of cytosolic  $\text{Ca}^{2+}$  (Figure 1C) measured by Fluo-4 (Figure 1B). The choice of these test

\* Correspondence: felix.althaus@vetpharm.uzh.ch

<sup>†</sup>Equal contributors

Institute of Pharmacology and Toxicology, University of Zurich-Vetsuisse, Winterthurerstrasse 260, Zurich CH-8057, Switzerland

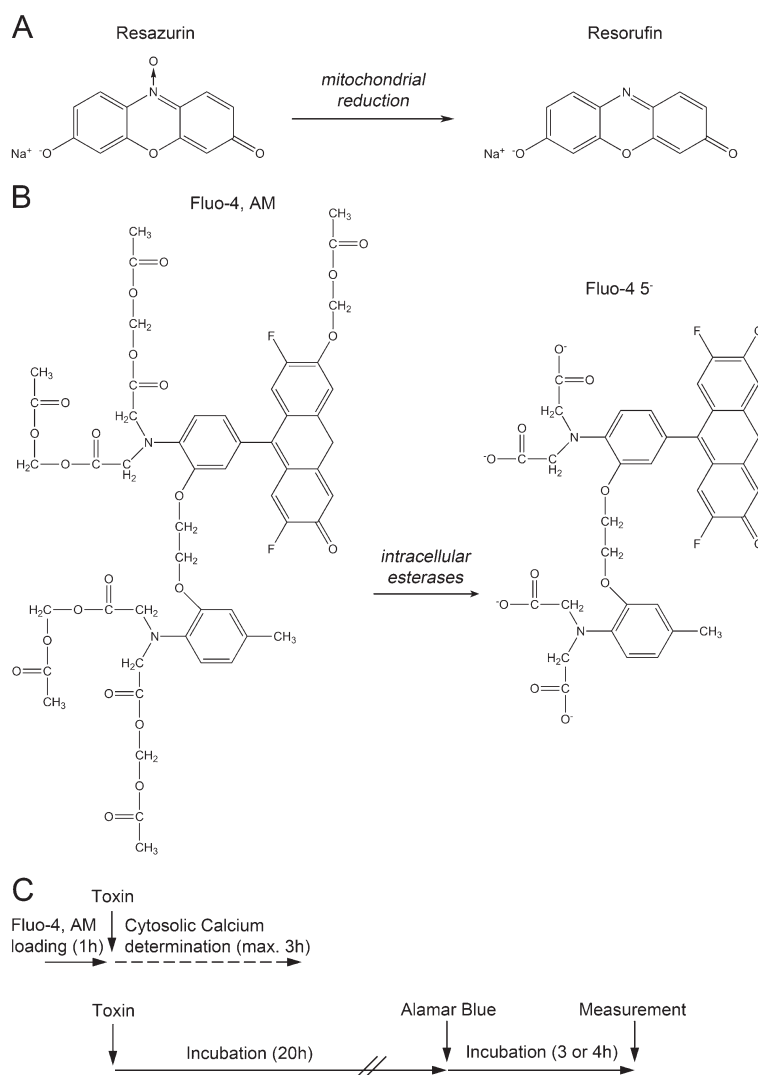
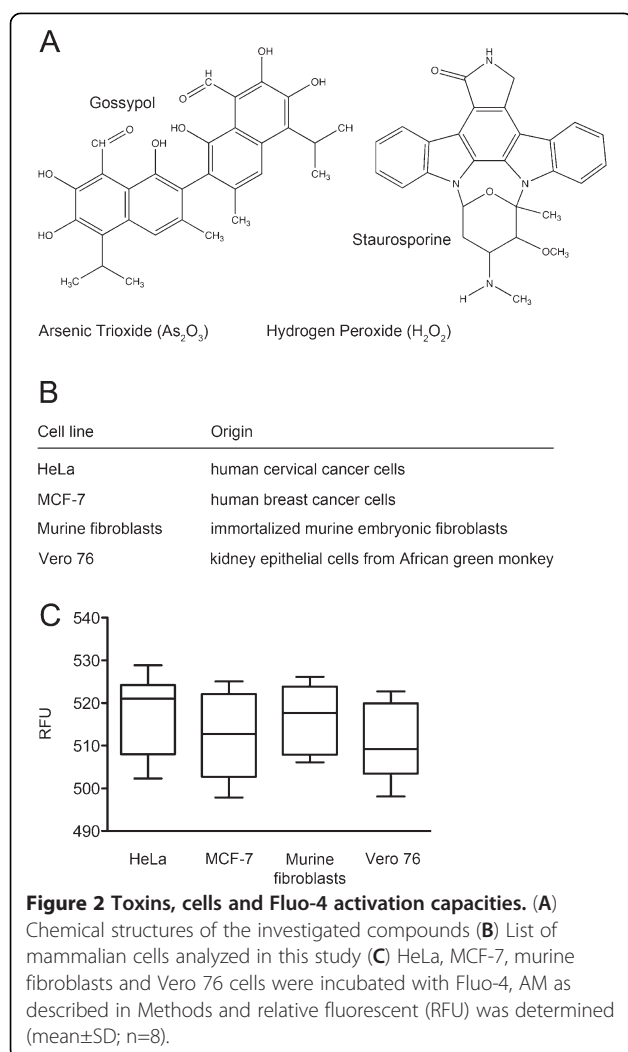


**Figure 1 Principle and experimental setup for cytotoxicity determination.** (A) Alamar Blue conversion (B) Principle of Fluo-4 assay for free cytosolic  $\text{Ca}^{2+}$  determination (C) Experimental time line for Fluo-4 and Alamar blue assays as investigated in this study.

compounds aims to cover a broad spectrum of different chemical structures and cytotoxicity mechanisms:

1.  $\text{As}_2\text{O}_3$  cytotoxicity is characterized by activation of the caspase cascade, simultaneous stress kinase signaling, the generation of reactive oxygen species (ROS) oxidizing macromolecules, and a disturbed endoplasmic reticulum function [9-13]. However, the detailed mechanisms by which arsenic interferes with living cells are not fully understood.
2. The racemic organic compound gossypol isolated from cotton seed and its metabolites display a wide pattern of cytotoxic cell alterations because of the complexity of gossypol chemistry and its potential chemical reactions with other macromolecules. Gossypol cytotoxicity includes ROS induction, microsomal enzyme inhibition, glutathione-S-transferase inhibition, mitochondrial dysfunction, caspase dependent and independent cell death associated with DNA degradation, and was described to interfere with the anti-apoptotic bcl-2 protein [14-18].
3. In this study,  $\text{H}_2\text{O}_2$  is used as surrogate for ROS. It oxidizes directly macromolecules including lipids, proteins and DNA. This can lead to a complex cytotoxicity response with the involvement of stress activated kinases, caspase and calpain activation, mitochondrial apoptosis induction factor (AIF) translocation, endoplasmic reticulum stress, nuclear poly(ADP-ribosylation), DNA degradation and many more [19-22].
4. The bacterial alkaloid staurosporine is intensively investigated as inducer of a classical apoptotic cell



death. It was initially described as an inhibitor of protein kinases [23-25]. On cellular level it leads to interruption of mitochondrial membranes, resulting in cytochrome c efflux and, as a consequence, to caspase dependent cell death [26-28].

The Alamar Blue assay was considered as a benchmark cytotoxicity test because of its improved performance compared to other pertinent assays, e.g. detection of cell densities as low as 200 cells/well [29,30]. Moreover, the Alamar Blue viability assay is suitable for high-throughput-screening (HTS) to identify cytotoxic compounds regardless of the chemical class and the underlying mechanism.

Changes in free cytosolic  $\text{Ca}^{2+}$  were investigated using the fluorescent  $\text{Ca}^{2+}$  binding dye Fluo-4 during the application of four toxins in all cell lines (Figure 1B). Cellular calcium levels are tightly regulated in cells. Under physiological conditions the  $\text{Ca}^{2+}$  concentration in the cytosol is several magnitudes below the  $\text{Ca}^{2+}$  in the extracellular space ( $10^{-7}$  M versus  $10^{-3}$  M, respectively [31]). Multiple

cellular  $\text{Ca}^{2+}$  stores contribute to the maintenance of  $\text{Ca}^{2+}$  homeostasis and virtually all cell organelles control the transport of  $\text{Ca}^{2+}$  across their membranes to regulate organelle/cellular function [31]. It is well established that imbalances in cellular  $\text{Ca}^{2+}$  homeostasis can lead to a variety of different cell stress responses including the induction of cell death [32].

In our study, we focussed on the sensitivity, the species-specificity and the limit of detection (LOD) of the Fluo-4  $\text{Ca}^{2+}$  assay. Sensitivity in our setting is defined as the ability to detect a significant effect of the used compounds at a specified concentration, whereas LOD is the lowest concentration level determined to be statistically different from blank. Here we show that  $\text{As}_2\text{O}_3$ , gossypol,  $\text{H}_2\text{O}_2$  and staurosporine induce a dose-dependent increase in cytosolic  $\text{Ca}^{2+}$  at lethal ( $\text{EC}_{75}$ ) and sublethal ( $\text{EC}_{25}$ ) concentrations immediately after application in all tested cell lines. The cytosolic  $\text{Ca}^{2+}$  elevation follows linear kinetics for the first 5 s under all test conditions. Cytosolic  $\text{Ca}^{2+}$  shifts occur independent of the chemical structure of the toxin in all tested cell systems and are persistent up to 3 h. Moreover, the increase of free cytosolic  $\text{Ca}^{2+}$  is detectable independent of the mode of cell death as investigated by caspase and PARP activity. Therefore, we suggest the determination of early cytosolic  $\text{Ca}^{2+}$  shifts as a rapid, highly efficient, inexpensive cytotoxicity test that is at least as sensitive as the established metabolic assay Alamar Blue.

## Results

### The $\text{Ca}^{2+}$ sensitive marker Fluo-4 is equally bio-activated in human, murine and monkey cells

Cytosolic  $\text{Ca}^{2+}$  was assessed using the fluorescence dye Fluo-4 (Figure 1B,C). This displays a high affinity to complex with  $\text{Ca}^{2+}$  ions ( $K_D$  of 345 nM) after its intracellular bio-activation by esterases [33]. Therefore, we first investigated the background fluorescence without any cytotoxic stress in HeLa, MCF-7, murine fibroblasts and Vero 76 cells to exclude any cell specific differences of Fluo-4, AM uptake and metabolism. We detected no differences between the tested cell lines under standard experiment conditions (Figure 2C).

### The $\text{EC}_{25}$ and $\text{EC}_{75}$ values of $\text{As}_2\text{O}_3$ , gossypol, $\text{H}_2\text{O}_2$ and staurosporine assessed in Alamar blue assays correlate with immediate cytosolic $\text{Ca}^{2+}$ rises in HeLa cells

We investigated the cytotoxic potential of the four toxins of interest in Alamar Blue viability assays as described in Methods (Figure 1A,C) and tested afterwards lethal and sublethal concentrations against changes in cytosolic  $\text{Ca}^{2+}$  homeostasis. The cytosolic  $\text{Ca}^{2+}$  levels remained unaffected for the whole measuring period in the absence of a toxic insult (Additional file 1A).

$\text{As}_2\text{O}_3$  reduced the cell viability of HeLa cells dose dependently in Alamar Blue assays (Figure 3A).  $\text{EC}_{25}$  and

EC<sub>75</sub> values of 5 and 50 μM were obtained, respectively. These concentrations were analyzed in Fluo-4 assays. Indeed, As<sub>2</sub>O<sub>3</sub> provoked a cytosolic Ca<sup>2+</sup> increase that was persistent until the end of the measurement (1800 s, Additional file 2A) in a dose-dependent fashion. Cytosolic Ca<sup>2+</sup> rose immediately after As<sub>2</sub>O<sub>3</sub> application and followed linear kinetics within the first 5 s (Figure 3A). The cytosolic Ca<sup>2+</sup> shifts differed significantly between 5 and 50 μM As<sub>2</sub>O<sub>3</sub> already at this early time point (2.4±1.94 RFU versus 7.7±2.78 RFU; Figure 3A). The differences in cytosolic Ca<sup>2+</sup> increases reflect the cytotoxicity values in Alamar Blue assays one day after toxin challenge, but already after 5 s.

Next, racemic gossypol was tested in Alamar Blue assays and compared with Fluo-4 analyses. Alamar Blue EC<sub>25</sub> (75 μM) as well as EC<sub>75</sub> (100 μM) induced cytosolic Ca<sup>2+</sup> shifts in HeLa cells (Figure 3B, Additional file 2B). The increase of cytosolic Ca<sup>2+</sup> signals was consistent for the whole period of observation (1800 s; 95.3±9.54 RFU versus 134.3±4.24 RFU, Additional file 2B). Interestingly, the Ca<sup>2+</sup> increases followed linear kinetics within the first 5 s after treatment and manifested dose dependent differences at this early time point (Figure 3B).

Similar results were obtained when HeLa cells were challenged with oxidative stress inducer H<sub>2</sub>O<sub>2</sub> (Figure 3C, Additional file 2C). 0.5 mM (EC<sub>25</sub>) and 2 mM (EC<sub>75</sub>) of H<sub>2</sub>O<sub>2</sub> were analyzed regarding cytosolic Ca<sup>2+</sup> imbalances. A dose dependency in the cytosolic Ca<sup>2+</sup> response was already significant within the first 5 s of measurements (Figure 3C) and it was maintained until the end of the experiments (Additional file 2C).

Staurosporine toxicity was analyzed in a similar way (Figure 3D, Additional file 2D). Again, 400 nM (EC<sub>25</sub>) and 1 μM (EC<sub>75</sub>) determined in Alamar Blue assays correlate with linear increases in cytosolic Ca<sup>2+</sup> levels for the first 5 s of Fluo-4 measurements (Figure 3D). In a next step, HeLa cells were challenged with doses below the EC<sub>25</sub> of the corresponding toxin. There were no differences detectable between the control and the As<sub>2</sub>O<sub>3</sub>, gossypol and staurosporine treated cells after 5 s (Additional file 1E). These results are identical to the data obtained with Alamar Blue assay after 24 h. Again, no significant difference was measured comparing the control cells with the As<sub>2</sub>O<sub>3</sub>, gossypol and staurosporine treated cells (Additional file 1F).

Additionally, we compared two structurally highly related titanium(IV)-salane complexes (Additional file 1G) for their toxicity in HeLa cells. As described earlier, both showed expected behaviour in Alamar Blue assay, i. e. cytotoxicity of TC52 and no impact on viability by TC53 [34]. These findings were reproduced in our assay, with enhanced cytosolic Ca<sup>2+</sup> fluxes at EC<sub>25</sub> and EC<sub>75</sub> in case of TC52, and no significant variation of cytosolic Ca<sup>2+</sup> levels by TC53 (Additional file 1H,I).

In a next set of experiments we tested the hypothesis that prolonged incubation with an established calcium

channel activator can also promote cell death due to an overload in free cytosolic Ca<sup>2+</sup> (Additional file 3). HeLa cells express purinergic P2X transmembranous Ca<sup>2+</sup> channels and a known ligand for this type of plasma membrane channels is ATP, but only when applied in the extracellular environment [35-38]. The toxicity of extracellular ATP is well established in a variety of cell types and was shown to be mediated by especially P2X<sub>7</sub> activation in HeLa cells [35,39-45]. Therefore we investigated the toxicity of ATP in this cell type and found that the EC<sub>25</sub> as well as the EC<sub>75</sub> deduced from Alamar blue assays (Additional file 3A) are reflected in dose dependent elevations of free cytosolic Ca<sup>2+</sup> when assessed with the Fluo-4 dye (Additional file 3B). Again, this continuous over activation of P2X and possibly others related channels due to the specific ligand ATP results in a linear increase in the Fluo-4 signal within the first 5 s of treatment (Additional file 3C).

#### **Early changes of cytosolic Ca<sup>2+</sup> accompany As<sub>2</sub>O<sub>3</sub>, gossypol, H<sub>2</sub>O<sub>2</sub> and staurosporine induced toxicity in MCF-7 cells**

We analyzed the toxicity of the four test compounds in the second human cell line MCF-7 (Figure 4A-D, Additional file 4A-D). The EC<sub>25</sub> and EC<sub>75</sub> concentrations of all toxins (20 μM and 50 μM As<sub>2</sub>O<sub>3</sub>, 60 μM and 75 μM gossypol, 5 mM and 10 mM H<sub>2</sub>O<sub>2</sub>, 0.2 μM and 0.4 μM staurosporine) were analyzed in Fluo-4 assays directly after application. Cytoplasmic Ca<sup>2+</sup> was not altered in untreated control MCF-7 cells within 2 h (Additional file 1B). All toxins generated a dose dependent increase in cytosolic Ca<sup>2+</sup> with linear kinetics within the first 5 s of the measurements (Figure 4A-D). Values at the EC<sub>25</sub> and EC<sub>75</sub> doses varied significantly not only at time point 5 s, but also for at least 30 min after the toxin treatment for all tested drugs (Additional file 4A-D).

#### **Drug-dependent elevations of cytosolic Ca<sup>2+</sup> indicate As<sub>2</sub>O<sub>3</sub>, gossypol, H<sub>2</sub>O<sub>2</sub> and staurosporine cytotoxicity in murine fibroblasts**

In the next set of experiments, the cytotoxicity of the drugs in murine fibroblasts was examined (Figure 5A-D, Additional file 5A-D). As expected, untreated control fibroblasts did not show any alteration in free cytosolic Ca<sup>2+</sup> levels (Additional file 1C).

Whereas 45 μM As<sub>2</sub>O<sub>3</sub> killed around 25% of murine fibroblasts, 50 μM represents the EC<sub>75</sub> value in the Alamar Blue assay one day after drug exposure. By using these concentrations in Fluo-4 assays, a linear increase of cytosolic Ca<sup>2+</sup> within the first 5 s in the presence of As<sub>2</sub>O<sub>3</sub> was detected (2.6±1.14 RFU versus 9.6±1.20 RFU). The cytoplasmic Ca<sup>2+</sup> slopes of the tested toxin concentrations were dose dependent and the RFUs at 5 s (Figure 5A) and 3 min (Additional file 5A) differed significantly between sublethal and lethal amounts of As<sub>2</sub>O<sub>3</sub>.

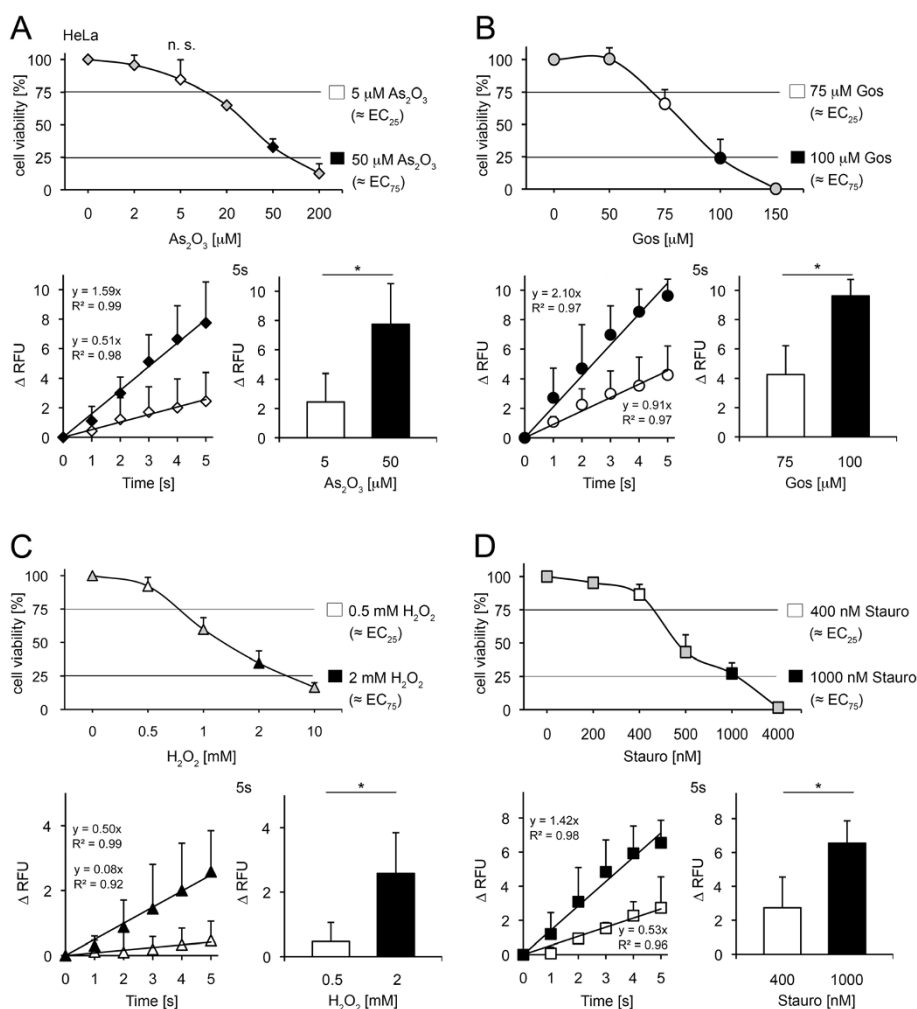


**Figure 3 Assessment of  $As_2O_3$ , gossypol,  $H_2O_2$  and staurosporine-induced toxicity in HeLa cells.** (A) Upper panel: Alamar Blue assay in presence of  $As_2O_3$  as indicated (mean $\pm$ SD;  $n \geq 3$ ; n.s. not significant;  $t$  test). Lower panel: Fluo-4 analysis of 5  $\mu M$  and 50  $\mu M$   $As_2O_3$  treated cells (mean $\pm$ SD;  $*p < 0.025$ ;  $n = 3$ ;  $t$  test) (B) Upper panel: Alamar Blue assay in presence of gossypol as indicated (mean $\pm$ SD;  $n \geq 3$ ). Lower panel: Fluo-4 analysis of 75  $\mu M$  and 100  $\mu M$  gossypol treated cells (mean $\pm$ SD;  $*p < 0.0025$ ;  $n \geq 4$ ;  $t$  test) (C) Upper panel: Alamar Blue assay in presence of  $H_2O_2$  as indicated (mean $\pm$ SD;  $n \geq 4$ ). Lower panel: Fluo-4 analysis of 0.5 mM and 2 mM  $H_2O_2$  treated cells (mean $\pm$ SD;  $*p < 0.025$ ;  $n \geq 3$ ;  $t$  test) (D) Upper panel: Alamar Blue assay in presence of staurosporine as indicated (mean $\pm$ SD;  $n \geq 3$ ). Lower panel: Fluo-4 analysis of 400 nM and 1000 nM staurosporine treated cells (mean $\pm$ SD;  $*p < 0.05$ ;  $n = 3$ ;  $t$  test).

Gossypol (75  $\mu M$  and 100  $\mu M$ ),  $H_2O_2$  (0.5 mM and 5 mM) and staurosporine (0.5  $\mu M$  and 4  $\mu M$ ) – concentration indicative of sublethal and lethal cell stress – were analysed in a similar way (Figure 5B-D, Additional file 5B-D). All these toxins confirmed a functional relationship between the applied dose and immediate alteration in cytoplasmic  $Ca^{2+}$  homeostasis. Moreover, the dose dependent differences in Fluo-4 determinations lasted up to 30 min post treatment (Additional file 5B,C). However, despite a significant rise in cytosolic  $Ca^{2+}$  level compared to control values at all time points tested, the observed increase between  $EC_{25}$  and  $EC_{75}$  was not statistically different after staurosporine treatment (Figure 5D and Additional file 5D).

### Determination of $As_2O_3$ , gossypol, $H_2O_2$ and staurosporine mediated cytotoxicity in Vero 76 cells

Vero 76 cells were analyzed in Fluo-4 assays using the  $EC_{25}$  and  $EC_{75}$  values for  $As_2O_3$ , gossypol,  $H_2O_2$  and staurosporine as assessed in Alamar Blue assays (Figure 6A-D, Additional file 6A-D). The cytosolic  $Ca^{2+}$  level remained robust during the whole analysis period without any toxic challenge (2 h, Additional file 1D).

Sublethal (35  $\mu M$ ) and lethal (100  $\mu M$ ) concentrations of  $As_2O_3$  were investigated in Fluo-4 assays (Figure 6A). A dose-dependent linear rise in cytosolic  $Ca^{2+}$  was observed within 5 s after toxin treatment ( $1.26 \pm 0.83$  RFU versus  $3.6 \pm 0.81$  RFU, Figure 6A). At this time point the cytosolic  $Ca^{2+}$  signals showed significant

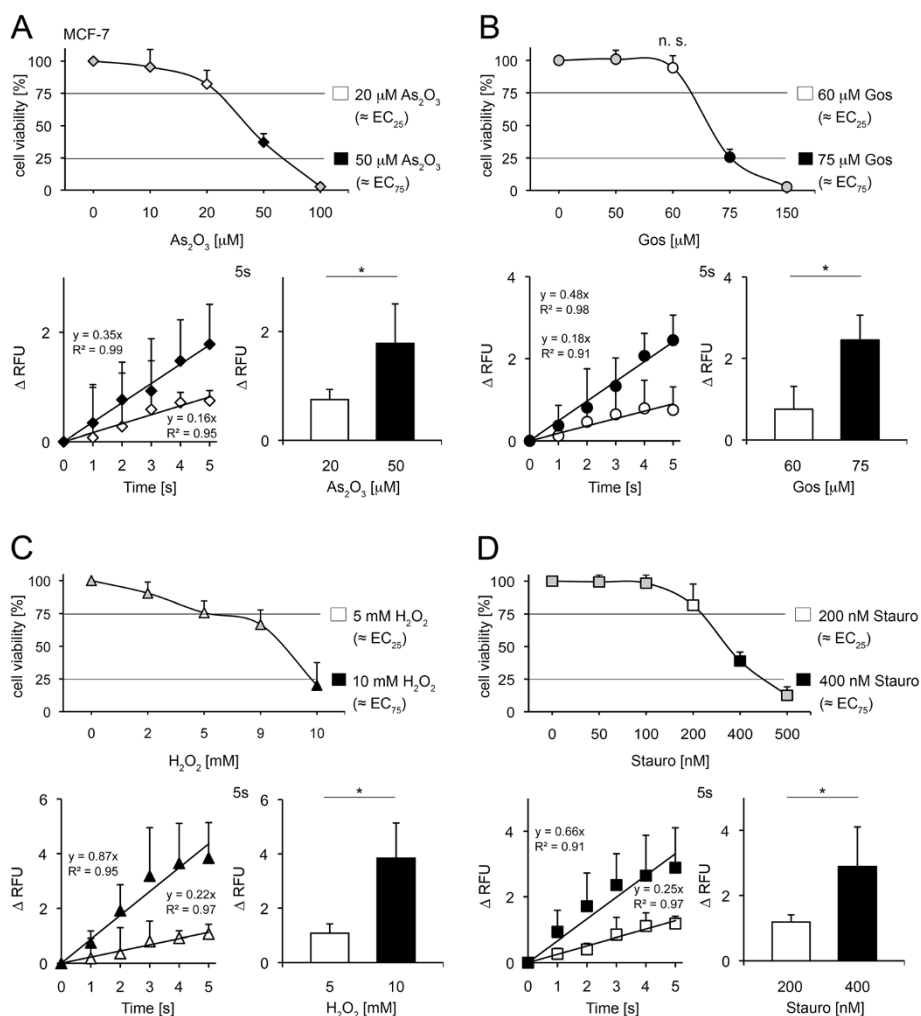


**Figure 4** Assessment of  $\text{As}_2\text{O}_3$ , gossypol,  $\text{H}_2\text{O}_2$  and staurosporine-induced toxicity in MCF-7 cells. (A) Upper panel: Alamar Blue assay in presence of  $\text{As}_2\text{O}_3$  as indicated (mean $\pm$ SD;  $n \geq 4$ ). Lower panel: Fluo-4 analysis of 20  $\mu\text{M}$  and 50  $\mu\text{M}$   $\text{As}_2\text{O}_3$  treated cells (mean $\pm$ SD; \* $p < 0.05$ ;  $n = 3$ ;  $t$  test) (B) Upper panel: Alamar Blue assay in presence of gossypol as indicated (mean $\pm$ SD;  $n \geq 4$ ; n.s. not significant;  $t$  test). Lower panel: Fluo-4 analysis of 60  $\mu\text{M}$  and 75  $\mu\text{M}$  gossypol treated cells (mean $\pm$ SD; \* $p < 0.025$ ;  $n = 4$ ;  $t$  test) (C) Upper panel: Alamar Blue assay in presence of  $\text{H}_2\text{O}_2$  as indicated (mean $\pm$ SD;  $n \geq 4$ ). Lower panel: Fluo-4 analysis of 5 mM and 10 mM  $\text{H}_2\text{O}_2$  treated cells (mean $\pm$ SD; \* $p < 0.005$ ;  $n \geq 3$ ;  $t$  test) (D) Upper panel: Alamar Blue assay in presence of staurosporine as indicated (mean $\pm$ SD;  $n \geq 4$ ). Lower panel: Fluo-4 analysis of 200 nM and 400 nM staurosporine treated cells (mean $\pm$ SD; \* $p < 0.05$ ;  $n \geq 3$ ;  $t$  test).

differences between the two doses, which were persistent until 3 h after drug exposure (Additional file 6A).

Gossypol toxicity was investigated at the concentrations of 75  $\mu\text{M}$  and 150  $\mu\text{M}$  in Vero 76 cells (Figure 6B). The increase of cytosolic  $\text{Ca}^{2+}$  following drug treatment was linear for both concentrations analysed in a dose dependent manner until 5 s post application. The fluorescence units were significantly different between 75  $\mu\text{M}$  and 100  $\mu\text{M}$  gossypol at this time point ( $1.4 \pm 0.71$  RFU versus  $4.2 \pm 1.12$  RFU). The difference in rise of cytosolic  $\text{Ca}^{2+}$  levels seen at 5 s was consistently maintained during the whole period of observation (3 min, 30 min and 3 h, Additional file 6B).

The  $\text{EC}_{25}$  (8.5 mM) and  $\text{EC}_{75}$  (10 mM) for  $\text{H}_2\text{O}_2$  in Vero 76 cells as assessed in Alamar Blue viability assays were investigated in Fluo-4 assays (Figure 6C).  $\text{H}_2\text{O}_2$  induced a very fast increase of cytosolic  $\text{Ca}^{2+}$  at the tested concentrations that was almost linear for the whole time of analysis (30 min, Additional file 6C). The free cytosolic  $\text{Ca}^{2+}$  elevations of  $\text{EC}_{25}$  and  $\text{EC}_{75}$  values were significantly different from control and displayed dose-dependent behaviour already 5 s after drug treatment (Figure 6C).

Comparable results were obtained when Vero 76 cells were challenged with 200 nM or 500 nM staurosporine respectively (Figure 6D, Additional file 6D). Again, as early as 5 s after toxin treatment the cytosolic  $\text{Ca}^{2+}$  reached

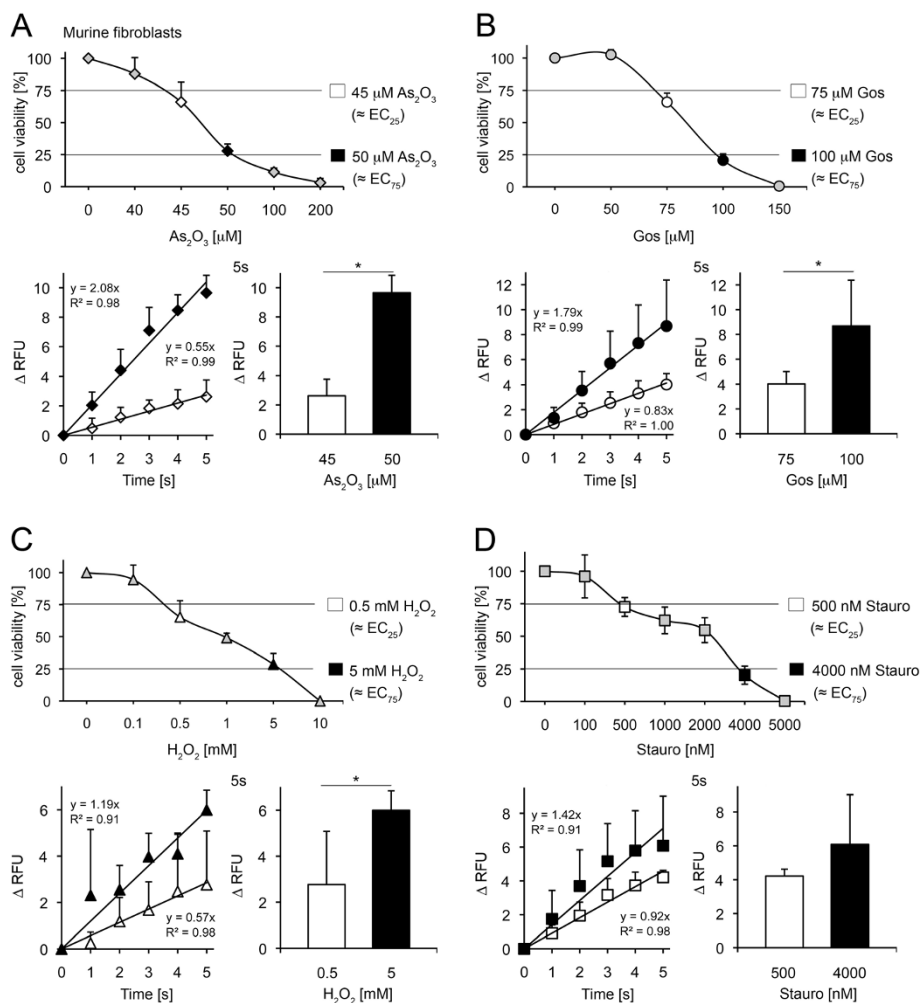


**Figure 5 Assessment of  $As_2O_3$ , gossypol,  $H_2O_2$  and staurosporine-induced toxicity in murine fibroblasts.** (A) Upper panel: Cells were treated with increasing concentrations of  $As_2O_3$  as indicated and afterwards cell viability was analysed with Alamar Blue (mean±SD;  $n \geq 4$ ). Lower panel: Fluo-4 analysis of 45  $\mu M$  and 50  $\mu M$   $As_2O_3$  treated cells (mean±SD;  $*p < 0.0001$ ;  $n \geq 4$ ; t test) (B) Upper panel: Cells were treated with increasing concentrations of gossypol as indicated and afterwards cell viability was analysed with Alamar Blue (mean±SD;  $n \geq 4$ ). Lower panel: Fluo-4 analysis of 75  $\mu M$  and 100  $\mu M$  gossypol treated cells (mean±SD;  $*p < 0.05$ ;  $n = 4$ ; t test) (C) Upper panel: Alamar Blue assay in presence of  $H_2O_2$  as indicated (mean±SD;  $n \geq 3$ ). Lower panel: Fluo-4 analysis of 0.5 mM and 5 mM  $H_2O_2$  treated cells (mean±SD;  $*p < 0.01$ ;  $n \geq 3$ ; t test) (D) Upper panel: Alamar Blue assay in presence of staurosporine as indicated (mean±SD;  $n \geq 3$ ). Lower panel: Fluo-4 analysis of 500 nM and 4000 nM staurosporine treated cells (mean±SD; n. s. not significant;  $n \geq 3$ ; t test).

significant differences between sublethal (200 nM) and lethal (500 nM) concentrations ( $1.1 \pm 0.43$  RFU versus  $5.0 \pm 0.83$  RFU) evident still at 3 h after drug application (Additional file 6D).

#### Immediate early drug-induced $Ca^{2+}$ shifts occur independent of the mode of cell death

We have identified cytosolic  $Ca^{2+}$  alterations as an early hallmark of cell death in all tested cell lines, regardless of species origin and of toxin (Figures 3, 4, 5 and 6). Next, we set out to elucidate the mode of cell death in the human cell lines HeLa and MCF-7. When treated with the equitoxic amounts ( $EC_{25}$  and  $EC_{75}$ ) of the four test compounds, caspase 7 and 9 were only processed in

HeLa cells into their active form as assessed by Western blot analysis 4 h after treatment (Figure 7A-D). By contrast, the cell death in MCF-7 cells was not mediated by activated caspases. The role of caspases in HeLa cells was confirmed by a parallel application of the caspase inhibitor Q-VD-OPh (20  $\mu M$ ) in Alamar Blue viability assays (Figure 7E). Q-VD-OPh could only interfere with  $As_2O_3$ ,  $H_2O_2$  and staurosporine-induced cell death, whereas gossypol-mediated viability reduction was not affected by caspase inhibition, despite their activation by all tested toxins and concentration (Figure 7A,C and D).

Next, we analysed nuclear PARP activity, which is induced immediately after genotoxic insult by binding to

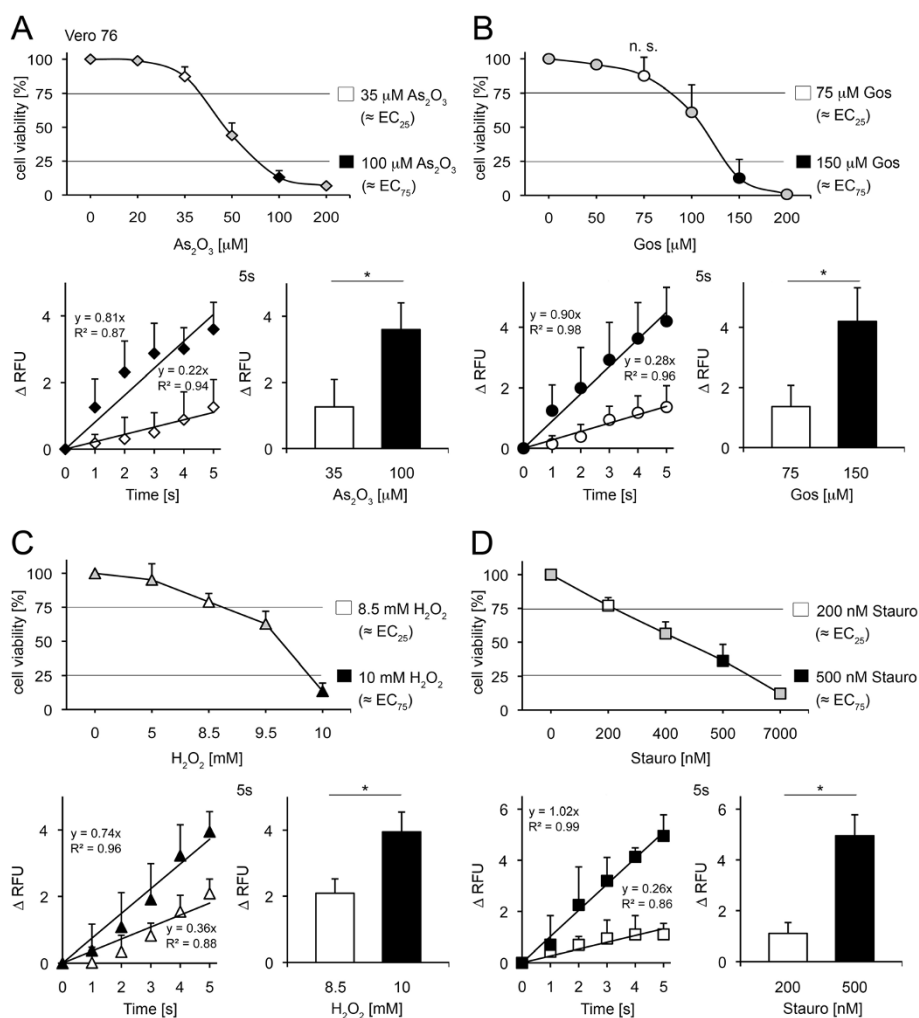


**Figure 6 Assessment of  $As_2O_3$ , gossypol,  $H_2O_2$  and staurosporine-induced toxicity in Vero 76 cells.** (A) Upper panel: Alamar Blue assay in presence of  $As_2O_3$  as indicated (mean $\pm$ SD;  $n\geq 3$ ). Lower panel: Fluo-4 analysis of 35  $\mu M$  and 100  $\mu M$   $As_2O_3$  treated cells (mean $\pm$ SD; \* $p < 0.025$ ;  $n = 3$ ;  $t$  test). (B) Upper panel: Alamar Blue assay in presence of gossypol as indicated (mean $\pm$ SD;  $n\geq 3$ ; n.s. not significant;  $t$  test). Lower panel: Fluo-4 analysis of 75  $\mu M$  and 150  $\mu M$  gossypol treated cells (mean $\pm$ SD; \* $p < 0.025$ ;  $n = 4$ ;  $t$  test) (C) Upper panel: Alamar Blue assay in presence of  $H_2O_2$  as indicated (mean $\pm$ SD;  $n\geq 3$ ). Lower panel: Fluo-4 analysis of 8.5 mM and 10 mM  $H_2O_2$  treated cells (mean $\pm$ SD; \* $p < 0.025$ ;  $n\geq 3$ ;  $t$  test) (D) Upper panel: Alamar Blue assay in presence of staurosporine as indicated (mean $\pm$ SD;  $n\geq 4$ ). Lower panel: Fluo-4 analysis of 200 nM and 500 nM staurosporine treated cells (mean $\pm$ SD; \* $p < 0.0025$ ;  $n = 3$ ;  $t$  test).

strand breaks [46,47]. Subsequent PAR formation accelerates repair processes [47-49], but if PAR is produced in excess due to cytotoxic drug concentrations it also promotes energy collapse, free cytosolic  $Ca^{2+}$  overload and the toxic translocation of apoptosis inducing factor (AIF) from mitochondria to the nucleus, leading finally to cell death [19-21,50]. Therefore, nuclear PAR accumulation was investigated 5 min after lethal ( $EC_{75}$ ) challenges with  $As_2O_3$ , gossypol,  $H_2O_2$  and staurosporine in both HeLa (Figure 8A) and MCF-7 cells (Figure 8B). Only the application of  $EC_{75}$  levels of  $H_2O_2$  but not of  $As_2O_3$ , gossypol and staurosporine caused detectable levels of nuclear PAR 5 min after treatment in immunofluorescence microscopy experiments. Interestingly, in HeLa cells the PARP

inhibitor PJ-34 could not only interfere with  $H_2O_2$ , but also with  $As_2O_3$ - and staurosporine-induced cell death (Figure 8C), pointing to PARP activity as a common feature in these different cell killing agents, even if PAR levels are below detection limit. By contrast, the application of PJ-34 was exclusively protective in  $H_2O_2$ -induced loss of viability in MCF-7 cells (Figure 8D). Gossypol-induced cell death was not affected by PARP inhibition in both tested cell lines.

## Discussion

The development of drugs and chemicals requires extensive cytotoxicity testing. Several tests rely on the energy status and the oxidative capacity of cells, i.e. the MTT

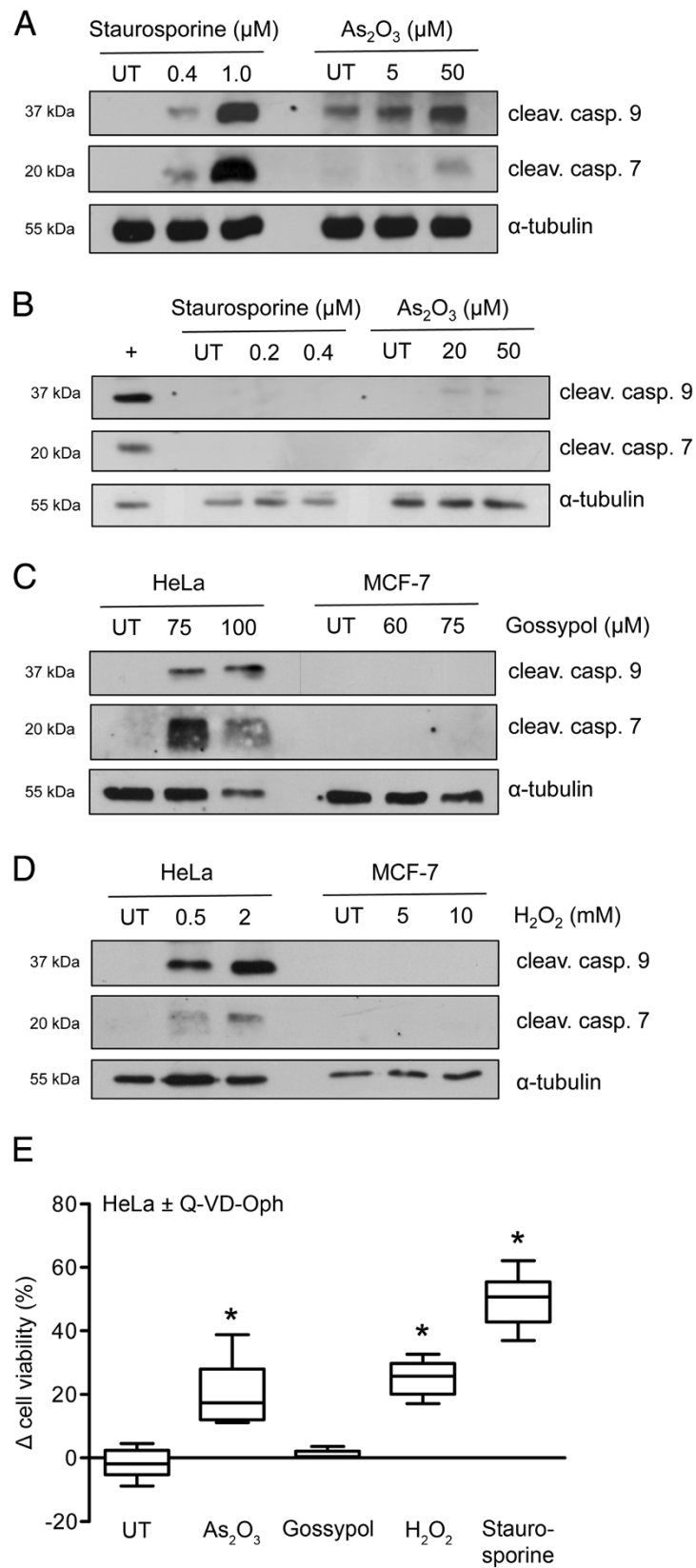


**Figure 7** (See legend on next page.)

(See figure on previous page.)

**Figure 7 Caspase activation after sublethal and lethal doses of As<sub>2</sub>O<sub>3</sub>, gossypol, H<sub>2</sub>O<sub>2</sub> and staurosporine in HeLa and MCF-7 cells.**

(A) Western blot analyses of cleaved caspase 7 and 9 after staurosporine and As<sub>2</sub>O<sub>3</sub> treatment in HeLa cells 4 h post treatment. A-tubulin is shown as loading control. (B) Western blot analyses of cleaved caspase 7 and 9 after staurosporine and As<sub>2</sub>O<sub>3</sub> treatment in MCF-7 cells 4 h post treatment. A-tubulin and 1 μM staurosporine treated HeLa cells are shown as controls. (C) Western blot analyses of cleaved caspase 7 and 9 after gossypol treatment as indicated in HeLa and MCF-7 cells 4 h post treatment with α-tubulin as loading control. (D) Western blot analyses of cleaved caspase 7 and 9 after H<sub>2</sub>O<sub>2</sub> treatment as indicated in HeLa and MCF-7 cells 4 h post treatment with α-tubulin as loading control. (E) Cell viability was assessed with Alamar Blue in HeLa cells in presence or absence of Q-VD-OPH (20 μM). Cells were challenged with EC<sub>75</sub> values of As<sub>2</sub>O<sub>3</sub>, gossypol, H<sub>2</sub>O<sub>2</sub> and staurosporine as indicated. Differences in cell survival of Q-VD-OPH plus toxin compared to toxin only treatment are shown (mean±SD; \*p<0.05; n=7; t test).

and the Alamar Blue assay [3]. Both can be applied in an automated way on multi-well plates for HTS. But there are certain limitations, as the final readout depends on two incubation steps: the exposure to the substance and the biotransformation of the reagent. Additionally, the cost effectiveness is a serious factor in large scale screening.

In recent publications, we reported a correlation between cytosolic Ca<sup>2+</sup> increase and cell death induced by oxidative stress [20,21]. Using a panel of different biological and pharmacological approaches we investigated distinct Ca<sup>2+</sup> sources merging in a composite pool of toxin dependent increase in free cytosolic Ca<sup>2+</sup>. The enzymatic activities of the nuclear PARP1 in conjunction with its counterpart poly(ADP-ribose) glycohydrolase (PARG) are responsible for extracellular Ca<sup>2+</sup> gated by transmembranous transient receptor mediated Ca<sup>2+</sup> channel (TRPM2). On the other hand, free cytosolic Ca<sup>2+</sup> origins also from intracellular sources. For instance, protein markers of endoplasmic reticulum (ER) stress were detected pointing to Ca<sup>2+</sup> released from ER stores in parallel. Blocking the influx of Ca<sup>2+</sup> protected the cells from oxidative insults.

In order to see whether Ca<sup>2+</sup> shifts are generally predictive of cytotoxicity, we investigated here a wide spectrum of toxins in cell lines from different species origin. The toxicity of arsenic trioxide, hydrogen peroxide, gossypol and staurosporine was tested in human, mouse, and monkey cells using Alamar Blue assay. These compounds have different cellular targets and induce different cell death pathways, ranging from general macromolecule damage, especially to DNA, by oxidative stressor H<sub>2</sub>O<sub>2</sub> to the apoptotic model compound staurosporine, which has been shown to inhibit a wide spectrum of kinases without damaging DNA. The toxicity data were compared to cytosolic Ca<sup>2+</sup> measurements at the respective sublethal (EC<sub>25</sub>) and lethal (EC<sub>75</sub>) doses. Our fluorimetric assay revealed in all settings a rapid rise in cytosolic Ca<sup>2+</sup>, regardless of species-origin and toxin applied. Moreover, it has a low LOD. Thus, our data provide evidence that Ca<sup>2+</sup> shifts are a common denominator in cytotoxic insults, independent of the mode of cell death. Interestingly, this can be monitored with an unmatched speed and at doses that show hardly significant changes in cell viability assays. Even sublethal (EC<sub>25</sub>) toxin concentrations generated slopes of free cytosolic Ca<sup>2+</sup>

increases significantly different from solvent controls indicative for the superior sensitivity of the Fluo-4 Ca<sup>2+</sup> assay. Moreover, this assay discriminates between structurally closely related titanium(IV)-salane complexes, i.e. toxic TC52 and non-toxic TC53. In an additional data set, we tested the toxicity of a physiological compound, i.e. ATP. High extracellular concentrations have been reported to induce cell death [35,39-45]. Indeed, we also detected free cytosolic Ca<sup>2+</sup> shifts in our assay after application of ATP in a similar setting as before (EC<sub>25</sub> and EC<sub>75</sub>). However, low dose extracellular ATP induces Ca<sup>2+</sup> shifts if cells express members of P2X and P2Y transporter family, as it is the case in HeLa cells [38]. Therefore, in this specific cell line and setting, we cannot rule out the occurrence of false-positives. Falsely categorizing a substance as positive or negative due to specific characteristics of the tested cells is always a risk in cytotoxicity screens. For example bleomycin, a well-established clastogenic agent and anti-tumor drug has to be taken up via the hCT2-transporter, which is the rate-limiting step determining its toxic activity as reviewed recently [51]. To avoid false-negative and false-positive results we suggest testing a panel of cell lines, which differ in their receptor repertoire. It can be expected that physiological molecules will obviously induce cellular responses including Ca<sup>2+</sup> dependent signaling processes. In contrast, engineered substances inducing a rise in free cytosolic Ca<sup>2+</sup> as presented in this study are indicative of unwanted biological effects. Therefore we conclude that cytosolic Ca<sup>2+</sup> increases within the first 5 s of exposure as measured with Fluo-4 dye are predictive of the cytotoxic potential of a xenobiotic compound.

## Conclusions

Our newly developed assay is applicable in cells from different species and with a wide variety of toxins, acting on different signaling pathways and modes of cell death. Measuring the free cytosolic Ca<sup>2+</sup> increase in the first 5 s of exposure shows the same or even higher statistical predictivity than the standard Alamar Blue assay. Thus, this fluorimetry-based method is a rapid predictor of cytotoxicity, superior to other assays in speed and cost effectiveness.

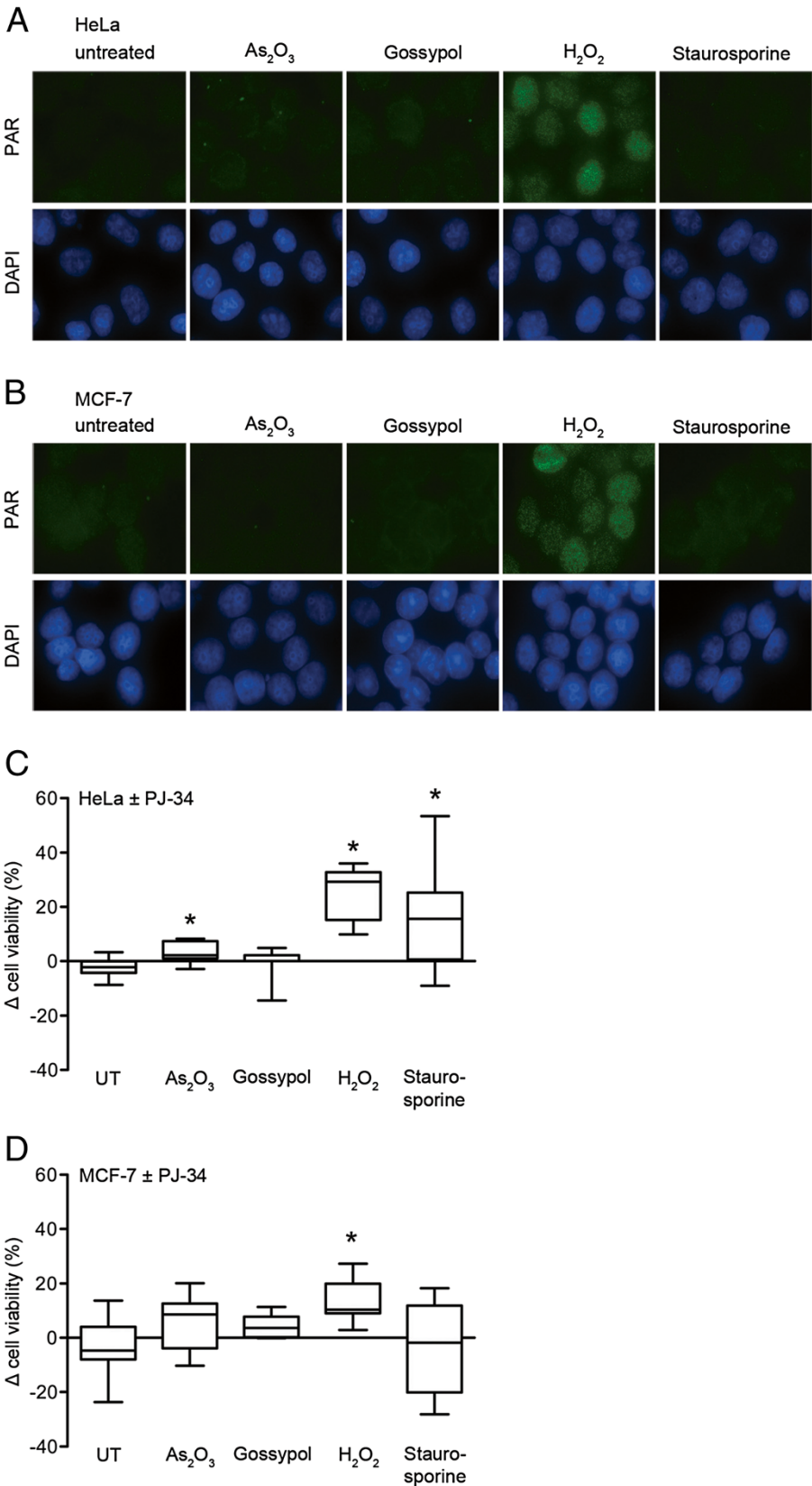


Figure 8 (See legend on next page.)

(See figure on previous page.)

**Figure 8 PAR formation and its effect on cell survival after lethal doses of As<sub>2</sub>O<sub>3</sub>, gossypol, H<sub>2</sub>O<sub>2</sub> and staurosporine in HeLa and MCF-7 cells.** (A) PAR detection by immunofluorescence in HeLa cells treated with 50 μM As<sub>2</sub>O<sub>3</sub>, 100 μM gossypol, 2 mM H<sub>2</sub>O<sub>2</sub> or 1 μM staurosporine as described in Methods. Nuclear DAPI staining is shown as control. (B) PAR detection by immunofluorescence in MCF-7 cells treated with 50 μM As<sub>2</sub>O<sub>3</sub>, 75 μM gossypol, 10 mM H<sub>2</sub>O<sub>2</sub> or 0.4 μM staurosporine as described with nuclear DAPI staining as control. (C) Cell viability was assessed with Alamar Blue in HeLa cells in presence or absence of PJ-34 (5 μM). Cells were challenged with EC<sub>75</sub> values of As<sub>2</sub>O<sub>3</sub>, gossypol, H<sub>2</sub>O<sub>2</sub> and staurosporine as indicated. Differences of cell survival are shown (mean±SD; \**p*<0.05; n=8; *t* test). (D) Cell viability was assessed with Alamar Blue in MCF-7 cells in presence or absence of PJ-34 (5 μM). Cells were challenged with EC<sub>75</sub> values of As<sub>2</sub>O<sub>3</sub>, gossypol, H<sub>2</sub>O<sub>2</sub> and staurosporine as indicated. Differences of cell survival are shown (mean±SD; \**p*<0.05; n=8; *t* test).

## Methods

### Cell culture

In this study HeLa, immortalized mouse embryonic fibroblasts, MCF-7 and Vero 76 cells were investigated (Figure 2B). All cell monolayers were cultured at 37°C in a water-saturated (5% CO<sub>2</sub>) atmosphere, in complete Dulbecco's modified Eagle's medium (D-MEM, Gibco, Lucerne, Switzerland) containing 1 g/L glucose and supplemented with 10% (v/v) FBS and Penicillin/Streptomycin (Invitrogen, Lucerne, Switzerland).

### Chemicals

*N*-(2-Quinolyl)valyl-aspartyl-(2,6-difluorophenoxy)methylketone (Q-VD-OPh) was from Calbiochem (Zug, Switzerland). *N*-(6-Oxo-5,6-dihydro-phenanthridin-2-yl)-*N,N*-dimethylacetamide, HCl (PJ-34) was obtained from ENZO Life Sciences (Lausen, Switzerland). HOECHST 33342 was from Invitrogen. Titanium(IV)-salane complexes TC52 and TC53 were both synthesized in the Chemistry Department (Thomas Huhn Group) of University of Konstanz/Germany. All other chemicals were from Applichem (Baden-Dättwil, Switzerland), Fluka (Buchs, Switzerland), Merck (Zug, Switzerland) or Sigma. All chemicals used as inhibitors were simultaneously administered with toxin treatment.

### Toxin treatment

Cells were challenged with 1 part (50 μL) H<sub>2</sub>O<sub>2</sub> (Sigma, Buchs, Switzerland) diluted in OPTI-MEM I (Gibco) to the desired concentration. After 1 h, 3 parts (150 μL) complete D-MEM were added. Gossypol (Sigma) was dissolved in DMSO to a stock solution of 100 mM. Then diluted in OPTI-MEM I to the desired concentration. Staurosporine (Sigma, dissolved in DMSO to a stock solution of 1 mM) and As<sub>2</sub>O<sub>3</sub> (Sigma, dissolved in H<sub>2</sub>O alkalized with NaOH to a stock solution of 5 mM) were diluted in D-MEM directly to the concentration needed. TC52 and TC53 were dissolved in DMSO to a stock solution of 2.5 mM and diluted in D-MEM to the desired concentration. ATP Mg<sup>2+</sup> salt (Sigma) was diluted in PBS supplemented with 2 mM Ca<sup>2+</sup> to the concentration needed. After 30 min of treatment the ATP solution was replaced with complete D-MEM. All

toxin treatments were maintained without any alterations until the end of the experiment.

### Alamar blue viability assay

Cells were seeded in 96-well-plates (15 000 cells/well) and incubated overnight (Figure 1C). Cells were treated with the toxins as described above. After 20 h (with TC52 and TC53 treatment 44 h), medium was replaced with 200 μL D-MEM 10% (v/v) Alamar Blue (Biozol, Eching, Germany). After 3 or 4 h, fluorescence was monitored at wavelength 530 nm for excitation and 590 nm for emission in LS55 luminescence spectrometer (Perkin-Elmer, Schwerzenbach, Switzerland).

### Calcium measurements

This was performed as described before [20]. Briefly, 20 000 cells/well in 96-well-plates (Costar Corning Incorporated, Baar, Switzerland) were washed twice with 49 parts of calcium-free HBSS (0.49 mM MgCl<sub>2</sub>, 0.41 mM MgSO<sub>4</sub>, 5.33 mM KCl, 0.44 mM KH<sub>2</sub>PO<sub>4</sub>, 4.17 mM NaHCO<sub>3</sub>, 137 mM NaCl, 0.34 mM Na<sub>2</sub>HPO<sub>4</sub>, 5.56 mM Dextrose) supplemented with 1 part 1 M HEPES (pH 7.2) (Assay Buffer) containing CaCl<sub>2</sub> or not. 100 μL Fluo-4-NW-dye-mix from Molecular Probes (Invitrogen) was added and incubated for 30 min at 37°C, followed by 30 min incubation in the dark at room temperature (Figure 1C). Changes in relative fluorescence units (ΔRFU) from the Fluo-4-NW-dye quantify alterations in free cytosolic Ca<sup>2+</sup> concentrations (excitation/emission 485/535 nm; slits 10/15 nm) in LS55 luminescence spectrometer (Perkin-Elmer) after toxin treatment. Stock solutions of toxins were diluted in Assay Buffer to the desired concentration. Free cytosolic Ca<sup>2+</sup> was monitored for the indicated time with a measure frequency of 1 s or less.

### Western blot detection

Immunoblots were performed as described previously [20]. The following primary antibodies were used: anti-cleaved-caspase-7 (Asp198, Cell Signaling; 1:1 000), anti-cleaved-caspase-9 (Asp315, Cell Signaling; 1:1 000) anti-α-Tubulin (Cell Signaling; 1:5 000). All secondary antibodies were from Sigma. Equal quantities of protein were loaded into each lane for SDS-PAGE separation as controlled by the simultaneous use of α-Tubulin as internal protein standards.

## Immunofluorescence of PAR

Cells were seeded on coverslips (Thermo Scientific, Allschwil, Switzerland) in 24-well-plates (Costar Corning Incorporated) and let attach overnight. The toxin treatment was performed in D-MEM for 5 min. Cells were fixed with ice-cold methanol and stored at  $-20^{\circ}\text{C}$  for 7 min. Coverslips were subsequently washed twice with 1xTris buffered saline (TBS, pH 7.4, 3 min at room temperature) and incubated with Blocking Buffer (1xTBS/0.2% Tween 20 (TBST), 1% BSA) for 30 min at  $37^{\circ}\text{C}$ . Monoclonal 10H anti-poly(ADP-ribose) (PAR) antibody [52] was used as 1<sup>st</sup> antibody (diluted 1:200 in Blocking Buffer). After an incubation for 1 h at  $37^{\circ}\text{C}$ , coverslips were washed three times with TBST (each 5 min), followed by a 2<sup>nd</sup> antibody incubation (Alexa Fluor 488-conjugated, 1:200 in blocking solution) for 1 h at  $37^{\circ}\text{C}$  in the dark. Afterwards, probes were washed three times with TBST (each 5 min). DAPI staining was performed for 5 min and coverslips were washed with  $\text{H}_2\text{O}$  and dried afterwards. The samples were further processed with ProLong Antifade kit (Invitrogen) according to the manufacturer's protocol and analyzed with a fluorescence microscope (Nikon) connected to a digital camera (Kappa, Grenchen, Switzerland).

## Statistical analysis

If not stated differently, all results are shown as mean $\pm$ SD of the indicated number of independent experiments. All statistical analyses were calculated with Prism Software 5.0b (GraphPad Software, San Diego California USA).

## Additional files

**Additional file 1: Control measurements of Fluo-4 free cytosolic calcium assay.** (A) HeLa cells (mean $\pm$ SD, n=2). (B) MCF-7 cells (mean $\pm$ SD, n=2). (C) Murine fibroblasts (mean $\pm$ SD, n=2). (D) Vero 76 cells (mean $\pm$ SD, n=3). (E)  $\text{Ca}^{2+}$  shift endpoint at 5 s after 1  $\mu\text{M}$ , 2  $\mu\text{M}$  or 5  $\mu\text{M}$   $\text{As}_2\text{O}_3$  with (mean $\pm$ SD; n $\geq$ 3; t test) compared to control in HeLa cells.  $\text{Ca}^{2+}$  shift endpoint at 5 s after 5  $\mu\text{M}$ , 10  $\mu\text{M}$  or 75  $\mu\text{M}$  gossypol with (mean $\pm$ SD; n $\geq$ 4; t test) compared to control.  $\text{Ca}^{2+}$  shift endpoint at 5 s after 100 nM, 200 nM or 400 nM staurosporine with (mean $\pm$ SD; n $\geq$ 3; t test) compared to control. (F) Alamar Blue endpoint at 24 h after 1  $\mu\text{M}$ , 2  $\mu\text{M}$  or 5  $\mu\text{M}$   $\text{As}_2\text{O}_3$  with (mean $\pm$ SD; n $\geq$ 3; t test) compared to control in HeLa cells. Alamar Blue endpoint at 24 h after 5  $\mu\text{M}$ , 10  $\mu\text{M}$  or 75  $\mu\text{M}$  gossypol with (mean $\pm$ SD; n $\geq$ 3; t test) compared to control. Alamar Blue endpoint at 24 h after 100 nM, 200 nM or 400 nM staurosporine with (mean $\pm$ SD; n $\geq$ 3; t test) compared to control. (G) Chemical structures of the investigated compounds TC52 and TC53. (H) Alamar Blue endpoint at 24 h after 4  $\mu\text{M}$  or 10  $\mu\text{M}$  TC52 or 10  $\mu\text{M}$  TC53 with (mean $\pm$ SD; n=3; t test) compared to control in HeLa cells (I)  $\text{Ca}^{2+}$  shift endpoint at 5 s after 4  $\mu\text{M}$  or 10  $\mu\text{M}$  TC52 or 10  $\mu\text{M}$  TC53 with (mean $\pm$ SD; n=3; t test) compared to untreated control in HeLa cells.

**Additional file 2: Impact of toxic compounds on cytosolic  $\text{Ca}^{2+}$  levels in HeLa cells.** (A)  $\text{Ca}^{2+}$  shifts after 5  $\mu\text{M}$  or 50  $\mu\text{M}$   $\text{As}_2\text{O}_3$  with (mean $\pm$ SD; \* $p$ <0.0005; n $\geq$ 3; t test) at 1800 s. (B)  $\text{Ca}^{2+}$  shifts after 75  $\mu\text{M}$  or 100  $\mu\text{M}$  gossypol with (mean $\pm$ SD; \* $p$ <0.0025; n=3; t test) at 1800 s. (C)  $\text{Ca}^{2+}$  shifts after 0.5 mM or 2 mM  $\text{H}_2\text{O}_2$  with (mean $\pm$ SD; \* $p$ <0.001; n $\geq$ 4; t test) at 180 s and (mean $\pm$ SD; \* $p$ <0.001; n $\geq$ 4; t test) at 1800 s. (D)  $\text{Ca}^{2+}$  shifts after 400 nM or 1000 nM staurosporine with (mean $\pm$ SD; \* $p$ <0.025; n=3; t test) at 1800 s.

**Additional file 3: Assessment of ATP-induced toxicity in HeLa cells.** (A) Alamar Blue assay in presence of ATP as indicated (mean $\pm$ SD; n $\geq$ 4).

(B)  $\text{Ca}^{2+}$  shifts after 25 mM or 40 mM ATP (mean $\pm$ SD; n $\geq$ 7). (C) Statistical evaluation of 25 or 40 mM ATP treated HeLa cells in Fluo-4 analyses (mean $\pm$ SD; \* $p$ <0.0005; n=7; t test).

**Additional file 4: Impact of toxic compounds on cytosolic  $\text{Ca}^{2+}$  levels in MCF-7 cells.** (A)  $\text{Ca}^{2+}$  shifts after 20  $\mu\text{M}$  or 50  $\mu\text{M}$   $\text{As}_2\text{O}_3$  with (mean $\pm$ SD; \* $p$ <0.01; n=3; t test) at 10800 s. (B)  $\text{Ca}^{2+}$  shifts after 60  $\mu\text{M}$  or 75  $\mu\text{M}$  gossypol with (mean $\pm$ SD; \* $p$ <0.001; n=3; t test) at 1800 s. (C)  $\text{Ca}^{2+}$  shifts after 5 mM or 10 mM  $\text{H}_2\text{O}_2$  with (mean $\pm$ SD; \* $p$ =0.0001; n $\geq$ 3; t test) at 1800 s. (D)  $\text{Ca}^{2+}$  shifts after 200 nM or 400 nM staurosporine with (mean $\pm$ SD; \* $p$ <0.01; n=3; t test) at 180 s and (mean $\pm$ SD; \* $p$ <0.005; n=3; t test) at 1800 s and (mean $\pm$ SD; \* $p$ <0.0025; n=3; t test) at 10800 s.

**Additional file 5: Impact of toxic compounds on cytosolic  $\text{Ca}^{2+}$  levels in murine fibroblasts.** (A)  $\text{Ca}^{2+}$  shifts after 45  $\mu\text{M}$  or 50  $\mu\text{M}$   $\text{As}_2\text{O}_3$  with (mean $\pm$ SD; \* $p$ <0.025; n=4; t test) at 180 s. (B)  $\text{Ca}^{2+}$  shifts after 75  $\mu\text{M}$  or 100  $\mu\text{M}$  gossypol with (mean $\pm$ SD; \* $p$ <0.025; n=3; t test) at 180 s and (mean $\pm$ SD; \* $p$ =0.0001; n=3; t test) at 1800 s. (C)  $\text{Ca}^{2+}$  shifts after 0.5 mM or 5 mM  $\text{H}_2\text{O}_2$  with (mean $\pm$ SD; \* $p$ <0.005; n $\geq$ 3; t test) at 180 s and (mean $\pm$ SD; \* $p$ <0.01; n $\geq$ 3; t test) at 1800 s. (D)  $\text{Ca}^{2+}$  shifts after 500 nM or 4000 nM staurosporine with (mean $\pm$ SD; not significant; n=3; t test) at 180 and 1800 s.

**Additional file 6: Impact of toxic compounds on cytosolic  $\text{Ca}^{2+}$  levels in Vero 76 cells.** (A)  $\text{Ca}^{2+}$  shifts after 35  $\mu\text{M}$  or 100  $\mu\text{M}$   $\text{As}_2\text{O}_3$  with (mean $\pm$ SD; \* $p$ <0.0025; n $\geq$ 3; t test) at 10800 s. (B)  $\text{Ca}^{2+}$  shifts after 75  $\mu\text{M}$  or 150  $\mu\text{M}$  gossypol with (mean $\pm$ SD; \* $p$ <0.025; n $\geq$ 3; t test) at 180 s with (mean $\pm$ SD; \* $p$ <0.005; n=3; t test) at 1800 s and (mean $\pm$ SD; \* $p$ <0.0001; n $\geq$ 3; t test) at 10800 s. (C)  $\text{Ca}^{2+}$  shifts after 8.5 mM or 10 mM  $\text{H}_2\text{O}_2$  with (mean $\pm$ SD; \* $p$ <0.005; n=3; t test) at 1800 s. (D)  $\text{Ca}^{2+}$  shifts after 200 nM or 500 nM staurosporine with (mean $\pm$ SD; \* $p$ <0.05; n=3; t test) at 10800 s.

## Competing interests

The authors declare that they have competing interests. A patent application protecting the invention has been filed (EP 12/187234).

## Authors' contribution

PW, CB and TP planned and performed the experiments. All authors analysed the data. PW, CB, SB and FRA wrote the manuscript. All authors read and approved the final manuscript.

## Acknowledgements

We thank Thomas Huhn from University of Konstanz for generously providing us with titanium(IV)-salane complexes TC52 and TC53. This work was supported by the Vetsuisse Faculty, and a grant from the Lotte and Adolf Hotz-Sprenger Foundation, Zurich, awarded to F. R. A.

Received: 14 September 2012 Accepted: 30 January 2013

Published: 6 February 2013

## References

- Williams ES, Panko J, Paustenbach DJ: **The european Union's REACH regulation: a review of its history and requirements.** *Crit Rev Toxicol* 2009, **39**:553–575.
- Hofer T, Gerner I, Gundert-Remy U, Liebsch M, Schulte A, Spielmann H, Vogel R, Wettig K: **Animal testing and alternative approaches for the human health risk assessment under the proposed new european chemicals regulation.** *Arch Toxicol* 2004, **78**:549–564.
- Sumantran VN: **Cellular chemosensitivity assays: an overview.** *Methods in molecular biology* 2011, **731**:219–236.
- Bradbury DA, Simmons TD, Slater KJ, Crouch SP: **Measurement of the ADP: ATP ratio in human leukaemic cell lines can be used as an indicator of cell viability, necrosis and apoptosis.** *J Immunol Methods* 2000, **240**:79–92.
- Burlinson B: **The in vitro and in vivo comet assays.** *Methods in molecular biology* 2012, **817**:143–163.
- Fields RD, Lancaster MV: **Dual-attribute continuous monitoring of cell proliferation/cytotoxicity.** *Am Biotechnol Lab* 1993, **11**:48–50.
- Nociari MM, Shalev A, Benias P, Russo C: **A novel one-step, highly sensitive fluorometric assay to evaluate cell-mediated cytotoxicity.** *J Immunol Methods* 1998, **213**:157–167.
- Nakayama GR, Caton MC, Nova MP, Parandoosh Z: **Assessment of the alamar blue assay for cellular growth and viability in vitro.** *J Immunol Methods* 1997, **204**:205–208.

9. Florea AM, Spletstoesser F, Busselberg D: **Arsenic trioxide (As<sub>2</sub>O<sub>3</sub>) induced calcium signals and cytotoxicity in two human cell lines: SY-5Y neuroblastoma and 293 embryonic kidney (HEK).** *Toxicol Appl Pharmacol* 2007, **220**:292–301.
10. Maeda H, Hori S, Ohizumi H, Segawa T, Kakehi Y, Ogawa O, Kakizuka A: **Effective treatment of advanced solid tumors by the combination of arsenic trioxide and L-buthionine-sulfoximine.** *Cell death and differentiation* 2004, **11**:737–746.
11. Shen L, Xu W, Li A, Ye J, Zhou J: **JWA enhances as(2)O(3)-induced tubulin polymerization and apoptosis via p38 in HeLa and MCF-7 cells.** *Apoptosis* 2011, **16**:1177–1193.
12. Cai BZ, Meng FY, Zhu SL, Zhao J, Liu JQ, Liu CJ, Chen N, Ye ML, Li ZY, Ai J, et al: **Arsenic trioxide induces the apoptosis in bone marrow mesenchymal stem cells by intracellular calcium signal and caspase-3 pathways.** *Toxicol Lett* 2010, **193**:173–178.
13. Tang CH, Chiu YC, Huang CF, Chen YW, Chen PC: **Arsenic induces cell apoptosis in cultured osteoblasts through endoplasmic reticulum stress.** *Toxicol Appl Pharmacol* 2009, **241**:173–181.
14. Sikora MJ, Bauer JA, Verhaegen M, Belbin TJ, Prystowsky MB, Taylor JC, Brenner JC, Wang S, Soengas MS, Bradford CR, Carey TE: **Anti-oxidant treatment enhances anti-tumor cytotoxicity of (–)-gossypol.** *Cancer Biol Ther* 2008, **7**:767–776.
15. Benz CC, Keniry MA, Ford JM, Townsend AJ, Cox FW, Palayoor S, Matlin SA, Hait WN, Cowan KH: **Biochemical correlates of the antitumor and antimitochondrial properties of gossypol enantiomers.** *Mol Pharmacol* 1990, **37**:840–847.
16. Arnold AA, Aboukameel A, Chen J, Yang D, Wang S, Al-Katib A, Mohammad RM: **Preclinical studies of apogossypolone: a new nonpeptidic pan small-molecule inhibitor of Bcl-2, Bcl-XL and Mcl-1 proteins in follicular small cleaved cell lymphoma model.** *Mol Cancer* 2008, **7**:20.
17. Balakrishnan K, Wierda WG, Keating MJ, Gandhi V: **Gossypol, a B<sub>H3</sub> mimetic, induces apoptosis in chronic lymphocytic leukemia cells.** *Blood* 2008, **112**:1971–1980.
18. Niu X, Li S, Wei F, Huang J, Wu G, Xu L, Xu D, Wang S: **Apogossypolone induces autophagy and apoptosis in breast cancer MCF-7 cells in vitro and in vivo.** *Breast Cancer* 2012.
19. Andrabi SA, Kim NS, Yu SW, Wang H, Koh DW, Sasaki M, Klaus JA, Otsuka T, Zhang Z, Koehler RC, et al: **Poly(ADP-ribose) (PAR) polymer is a death signal.** *Proc Natl Acad Sci U S A* 2006, **103**:18308–18313.
20. Blenn C, Wyrsch P, Bader J, Bollhalder M, Althaus FR: **Poly(ADP-ribose) glycohydrolase is an upstream regulator of Ca<sup>2+</sup> fluxes in oxidative cell death.** *Cellular and molecular life sciences: CMLS* 2011, **68**:1455–1466.
21. Wyrsch P, Blenn C, Bader J, Althaus FR: **Cell death and autophagy under oxidative stress: roles of poly(ADP-ribose) polymerases and Ca<sup>2+</sup>.** *Mol Cell Biol* 2012, **17**:3541–3553.
22. Choi SE, Min SH, Shin HC, Kim HE, Jung MW, Kang Y: **Involvement of calcium-mediated apoptotic signals in H<sub>2</sub>O<sub>2</sub>-induced MIN6N8a cell death.** *Eur J Pharmacol* 2006, **547**:1–9.
23. Tamaoki T, Nomoto H, Takahashi I, Kato Y, Morimoto M, Tomita F: **Staurosporine, a potent inhibitor of phospholipid/Ca<sup>++</sup>-dependent protein kinase.** *Biochem Biophys Res Commun* 1986, **135**:397–402.
24. Ruegg UT, Burgess GM: **Staurosporine, K-252 and UCN-01: potent but nonspecific inhibitors of protein kinases.** *Trends Pharmacol Sci* 1989, **10**:218–220.
25. Herbert JM, Seban E, Maffrand JP: **Characterization of specific binding sites for [3H]-staurosporine on various protein kinases.** *Biochem Biophys Res Commun* 1990, **171**:189–195.
26. Kruman I, Guo Q, Mattson MP: **Calcium and reactive oxygen species mediate staurosporine-induced mitochondrial dysfunction and apoptosis in PC12 cells.** *J Neurosci Res* 1998, **51**:293–308.
27. Zhu Y, Zhao L, Liu L, Gao P, Tian W, Wang X, Jin H, Xu H, Chen Q: **Beclin 1 cleavage by caspase-3 inactivates autophagy and promotes apoptosis.** *Protein Cell* 2010, **1**:468–477.
28. Van den Broeke C, Radu M, Nauwynck HJ, Chernoff J, Favoreel HW: **Role of group a p21-activated kinases in the anti-apoptotic activity of the pseudorabies virus US3 protein kinase.** *Virus Res* 2011, **155**:376–380.
29. Hamid R, Rotshteyn Y, Rabadi L, Parikh R, Bullock P: **Comparison of alamar blue and MTT assays for high through-put screening.** *Toxicol In Vitro* 2004, **18**:703–710.
30. Page B, Page M, Noel C: **A new fluorometric assay for cytotoxicity measurements in-vitro.** *Int J Oncol* 1993, **3**:473–476.
31. Michelangeli F, Ogunbayo OA, Wootton LL: **A plethora of interacting organellar Ca<sup>2+</sup> stores.** *Curr Opin Cell Biol* 2005, **17**:135–140.
32. Orrenius S, Nicotera P, Zhivotovskiy B: **Cell death mechanisms and their implications in toxicology.** *Toxicological sciences: an official journal of the Society of Toxicology* 2011, **119**:3–19.
33. Hansen KB, Brauner-Osborne H: **FLIPR assays of intracellular calcium in GPCR drug discovery.** *Methods Mol Biol* 2009, **552**:269–278.
34. Immel TA, Debiak M, Groth U, Burkle A, Huhn T: **Highly selective apoptotic cell death induced by halo-salane titanium complexes.** *Chem Med Chem* 2009, **4**:738–741.
35. Wang Q, Li X, Wang L, Feng YH, Zeng R, Gorodeski G: **Antiapoptotic effects of estrogen in normal and cancer human cervical epithelial cells.** *Endocrinology* 2004, **145**:5568–5579.
36. Ralevic V, Burnstock G: **Receptors for purines and pyrimidines.** *Pharmacol Rev* 1998, **50**:413–492.
37. Liu PS, Chiung YM, Kao YY, Chen HT: **2,4-Toluene diisocyanate suppressed the calcium signaling of ligand gated ion channel receptors.** *Toxicology* 2006, **219**:167–174.
38. Welter-Stahl L, da Silva CM, Schachter J, Persechini PM, Souza HS, Ojcius DM, Coutinho-Silva R: **Expression of purinergic receptors and modulation of P2X7 function by the inflammatory cytokine IFN $\gamma$  in human epithelial cells.** *Biochim Biophys Acta* 2009, **1788**:1176–1187.
39. Zheng LM, Zychlinsky A, Liu CC, Ojcius DM, Young JD: **Extracellular ATP as a trigger for apoptosis or programmed cell death.** *The Journal of cell biology* 1991, **112**:279–288.
40. Gulbransen BD, Bashashati M, Hirota SA, Gui X, Roberts JA, MacDonald JA, Muruve DA, McKay DM, Beck PL, Mawe GM, et al: **Activation of neuronal P2X7 receptor-pannexin-1 mediates death of enteric neurons during colitis.** *Nature medicine* 2012, **18**:600–604.
41. Di Virgilio F, Chiozzi P, Falzoni S, Ferrari D, Sanz JM, Venketaraman V, Baricordi OR: **Cytolytic P2X purinoceptors.** *Cell death and differentiation* 1998, **5**:191–199.
42. Chow SC, Kass GE, Orrenius S: **Purines and their roles in apoptosis.** *Neuropharmacology* 1997, **36**:1149–1156.
43. Hanley PJ, Kronlage M, Kirschning C, del Rey A, Di Virgilio F, Leipziger J, Chessell IP, Sargin S, Filippov MA, Lindemann O, et al: **Transient P2X7 receptor activation triggers macrophage death independent of toll-like receptors 2 and 4, caspase-1, and pannexin-1 proteins.** *J Biol Chem* 2012, **287**:10650–10663.
44. Mirabelli F, Bellomo G, Nicotera P, Moore M, Orrenius S: **Ca<sup>2+</sup> Homeostasis and cytotoxicity in isolated hepatocytes: studies with extracellular adenosine 5'-triphosphate.** *J Biochem Toxicol* 1986, **1**:29–39.
45. Kawano A, Tsukimoto M, Noguchi T, Hotta N, Harada H, Takenouchi T, Kitani H, Kojima S: **Involvement of P2X4 receptor in P2X7 receptor-dependent cell death of mouse macrophages.** *Biochem Biophys Res Commun* 2012, **419**:374–380.
46. Dantzer F, Ame JC, Schreiber V, Nakamura J, Menissier-de Murcia J, de Murcia G: **Poly(ADP-ribose) polymerase-1 activation during DNA damage and repair.** *Methods Enzymol* 2006, **409**:493–510.
47. Malanga M, Althaus FR: **The role of poly(ADP-ribose) in the DNA damage signaling network.** *Biochem Cell Biol* 2005, **83**:354–364.
48. Realini CA, Althaus FR: **Histone shuttling by poly(ADP-ribosylation).** *J Biol Chem* 1992, **267**:18858–18865.
49. Wang Z, Wang F, Tang T, Guo C: **The role of PARP1 in the DNA damage response and its application in tumor therapy.** *Front Med* 2012, **6**:156–164.
50. Cohausz O, Blenn C, Malanga M, Althaus FR: **The roles of poly(ADP-ribose)-metabolizing enzymes in alkylation-induced cell death.** *Cellular and molecular life sciences: CMLS* 2008, **65**:644–655.
51. Aouida M, Ramotar D: **A new twist in cellular resistance to the anticancer drug bleomycin-A5.** *Curr Drug Metab* 2010, **11**:595–602.
52. Kawamitsu H, Hoshino H, Okada H, Miwa M, Momoi H, Sugimura T: **Monoclonal antibodies to poly(adenosine diphosphate ribose) recognize different structures.** *Biochemistry-US* 1984, **23**:3771–3777.

doi:10.1186/1478-811X-11-11

Cite this article as: Wyrsch et al.: Cytosolic Ca<sup>2+</sup> shifts as early markers of cytotoxicity. *Cell Communication and Signaling* 2013 **11**:11.